Left/right asymmetrically expressed ephrin and Flamingo proteins regulate lateralized axon growth in C. elegans

Khulganaa Buyannemekh, Paul Villoutreix, Vincent Bertrand

Developmental Biology 517 (2025) 117–125

Contents lists available at ScienceDirect

Developmental Biology

journal homepage: www.elsevier.com/locate/developmentalbiology

Original research article

Left/right asymmetrically expressed ephrin and Flamingo proteins regulate lateralized axon growth in *C. elegans*

Khulganaa Buyannemekh [a,b,c], Paul Villoutreix [b,c], Vincent Bertrand [a,*]

[a] Aix Marseille Univ, CNRS, IBDM, Turing Center for Living Systems, Marseille, France
[b] Aix Marseille Univ, Université de Toulon, CNRS, LIS, Turing Centre for Living Systems, Marseille, France
[c] Aix Marseille Univ, INSERM, MMG, Turing Centre for Living Systems, Marseille, France

ARTICLE INFO

Keywords:
Left-right asymmetry
Nervous system development
Axon guidance
Ephrin
Flamingo
C. elegans

ABSTRACT

While the nervous system of bilaterian animals is mainly left-right (L-R) symmetric at the anatomical level, some molecular and functional L-R asymmetries exist. However, the extent of these molecular asymmetries and their functional consequences remain poorly characterized. *C. elegans* allows to study L-R asymmetries in the nervous system with single-neuron resolution. We have previously shown that a neural bHLH transcription factor, HLH-16/Olig, is L-R asymmetrically expressed in the AIY neuron lineage and regulates AIY axon projections in a L-R asymmetric manner. Here, by combining a candidate approach and single-cell RNA sequencing data analysis, we identify the ephrin protein EFN-2 and the Flamingo protein FMI-1 as downstream targets of HLH-16 that are L-R asymmetrically expressed in the AIY lineage. We show that EFN-2 and FMI-1 collaborate in the L-R asymmetric regulation of axonal growth. EFN-2 may act via a non-canonical receptor of the L1CAM family, SAX-7. Our study reveals novel molecular L-R asymmetries in the *C. elegans* nervous system and their functional consequences.

1. Introduction

In bilaterian animals, the nervous system is mainly left-right (L-R) symmetric. However, some L-R asymmetries exist at structural, molecular and functional levels (Concha et al., 2012; Duboc et al., 2015; Gunturkun and Ocklenburg, 2017; Sun and Walsh, 2006). These asymmetries are important in animal behaviors and defects in the lateralization of the nervous system are associated with neurological disorders in humans, such as dyslexia or schizophrenia (Concha et al., 2012; Duboc et al., 2015; Gunturkun and Ocklenburg, 2017; Sun and Walsh, 2006). Examples of morphological asymmetries include the Sylvian fissure in humans, the epithalamus in zebrafish, the asymmetrical body in *Drosophila* and unilateral neurons in *C. elegans* (Duboc et al., 2015; Geminard et al., 2014; Hobert et al., 2002; Sun and Walsh, 2006). In addition, even structures that are morphologically bilaterally symmetric can display molecular and functional L-R asymmetries as illustrated with the pairs of ASE and AWC neurons in *C. elegans* (Alqadah et al., 2016; Hobert, 2014). However, the extent of molecular and functional asymmetries in animal nervous systems remains poorly characterized.

C. elegans is a good system to study nervous system lateralization as the position, connectivity and lineage of every neuron have been mapped (Sulston and Horvitz, 1977; Sulston et al., 1983; White et al., 1986). L-R asymmetries in the nervous system can therefore be studied with single-cell resolution. Although the *C. elegans* nervous system is mainly bilaterally symmetric, some morphological L-R asymmetries exist, such as unilateral neurons, asymmetric axonal projections or asymmetric cell body positions (Hobert et al., 2002). In addition, even morphologically symmetric neuronal pairs can display molecular and functional L-R asymmetries. The two best characterized examples are the gustatory neurons ASE and the olfactory neurons AWC. The left ASE and right ASE neurons express different chemoreceptors, which allows them to sense different chemicals (Hobert, 2014). This directional asymmetry is induced early during development, at 4-cell stage, by an asymmetric Notch signaling event (Hobert, 2014). In contrast, AWC asymmetry is not directional but stochastic (Alqadah et al., 2016). Interactions between the two AWC neurons, involving gap junctions and calcium signaling, lead to activation of the expression of the *str-2* chemoreceptor gene in only one of the AWC neurons, while the other expresses *srsx-3* (Alqadah et al., 2016). Consequently, the two AWC neurons sense different chemicals. A third, less characterized example is the AIY neurons. AIY is a pair of cholinergic interneurons, one neuron located on the left side (AIYL) and the other on the right side (AIYR). The two AIY neurons are L-R symmetric in terms of position, axonal projection and lineage. We have previously observed that during embryonic

* Corresponding author.
E-mail address: vincent.bertrand@univ-amu.fr (V. Bertrand).

https://doi.org/10.1016/j.ydbio.2024.09.014
Received 29 July 2024; Received in revised form 22 September 2024; Accepted 25 September 2024
Available online 26 September 2024

development, a bHLH transcription factor of the Olig family, HLH-16, is asymmetrically expressed in the AIY lineage (Bertrand et al., 2011). HLH-16 is expressed in the AIY grandmother cells and their progeny (that generate the AIY interneurons and SMDD, SIAD and SIBV motoneurons) with higher expression levels on the left side (Fig. 1A). This asymmetry is generated, independently of ASE and AWC asymmetries, by a late Notch signaling event during gastrulation. Interestingly, in *hlh-16* loss-of-function mutants, the AIY axon stops prematurely, and this defect is stronger in AIYL than AIYR, suggesting that higher levels of HLH-16 expression are required in the left lineage for correct axonal projection. However, how HLH-16 regulates this asymmetric axonal growth process is unknown. We expect the presence of asymmetrically expressed regulators of axonal growth downstream of HLH-16. This suggests that novel molecular asymmetries remain to be discovered in the *C. elegans* nervous system.

In this study, using both single-cell RNA-sequencing (scRNA-seq) data analysis and a candidate approach, we identify the ephrin protein EFN-2 and the Flamingo protein FMI-1 as L-R asymmetrically expressed in the AIY lineage. We show that these asymmetries are controlled by HLH-16, and that EFN-2 and FMI-1 cooperate to regulate AIY axonal growth in an asymmetric manner. We also identify the L1CAM protein SAX-7 as a putative non-canonical receptor for EFN-2 in this process. Our study reveals a L-R asymmetric molecular program regulating the formation of morphologically symmetric axons.

2. Materials and methods

2.1. Genetics

All analyses were performed on *C. elegans* hermaphrodites grown at 20 °C. Strain maintenance and genetic crosses were conducted following standard protocols (Stiernagle, 2006).

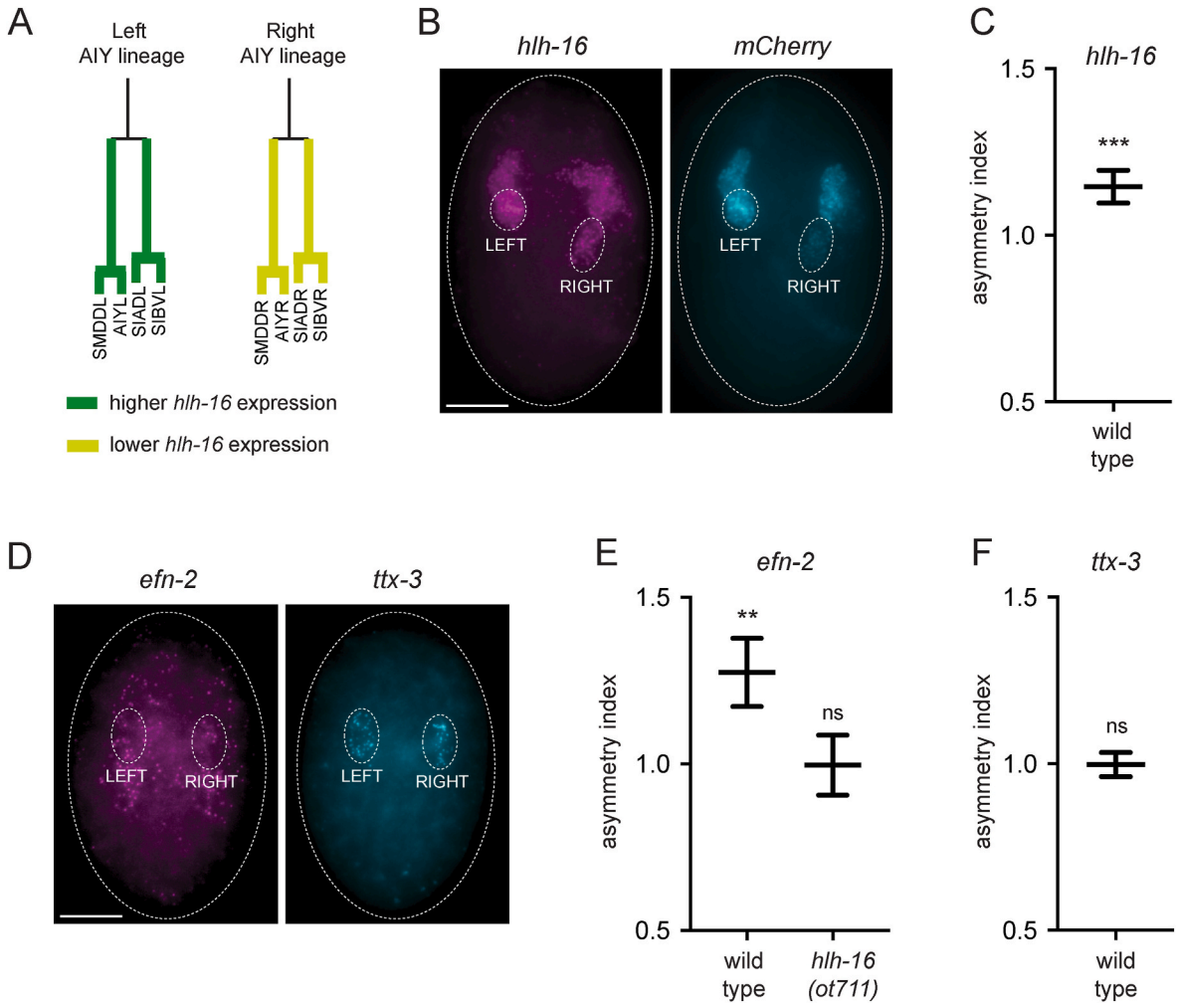

Fig. 1. Asymmetric expression of *hlh-16* and *efn-2*.
(A) Left and Right AIY lineages with asymmetric expression of *hlh-16* reporters. (B) Image of an embryo labeled with smFISH targeting endogenous *hlh-16* mRNAs (Quasar 670) and *mCherry* mRNAs (CAL Fluor Red 610). *mCherry* was used to identify the AIY grandmother cells with the *hlh-16p::mCherry* transgene (*stIs10546*), where *mCherry* expression is driven by the *hlh-16* promoter. Left and right AIY grandmother cells are circled, anterior is up, scale bar: 10 μm. (C) Asymmetry index of *hlh-16* mRNA numbers detected by smFISH in the AIY grandmother cell. The asymmetry index is defined as the number of mRNAs in the left cell divided by the mean number of mRNAs of the two cells. This index varies between 2 (for a gene expressed only in the left cell) and 0 (for a gene expressed only in the right cell), with a value of 1 for a symmetrically expressed gene. n = 21 embryos analyzed, bars represent the mean and SEM, comparison to 1 using Wilcoxon signed-rank test (***$p < 0.005$). (D) Image of an embryo labeled with smFISH targeting *efn-2* mRNAs (Quasar 670) and *ttx-3* mRNAs (CAL Fluor Red 610). *ttx-3* was used to identify the AIY mother cells. Left and right AIY mother cells are circled, anterior is up, scale bar: 10 μm. (E) Asymmetry index of *efn-2* mRNA numbers detected by smFISH in the AIY mother cell. n = 30 embryos analyzed for wild-type and 29 embryos for *hlh-16(ot711)* mutants, bars represent the mean and SEM, comparison to 1 using Wilcoxon signed-rank test (**$p < 0.01$, ns - not significant). (F) Asymmetry index of *ttx-3* mRNA numbers detected by smFISH in the AIY mother cell. n = 30 embryos analyzed, bars represent the mean and SEM, comparison to 1 using Wilcoxon signed-rank test (ns - not significant).

2.2. smFISH

The smFISH procedure was adapted from a previously developed protocol (Bolkova and Lanctot, 2016) as described in (Bordet et al., 2022).

smFISH probes were designed using the Stellaris Custom Probe Designer (https://www.biosearchtech.com/stellaris-designer) and ordered from BioCat GmbH. The probe sets contained 25–48 probes (each 20 nt long) targeting the mRNA sequence of the gene of interest. The probes were coupled with either Quasar 670, Quasar 570 or CAL Fluor Red 610 dyes. The probe sequences are listed in Table S1.

smFISH experiments were conducted on *C. elegans* embryos fixed at 250–460 min post fertilization. This time window corresponds to embryos at early to 1.5-fold stage of embryogenesis and covers the last two cell divisions of the AIY lineage. This allowed us to target the grandmother, mother and terminal SMDD and AIY neurons. We used the pulse-lay method to synchronize and stage the embryos. Adult gravid hermaphrodites were placed on a new agar plate and allowed to lay eggs for 1 h. The adults were removed, and the embryos were incubated at 20 °C until the stage of interest. They were harvested by suspension in water, followed by washes and centrifugation.

We used the freeze-cracking method to break the eggshell and permeabilize the embryos for fixation and hybridization. The harvested embryos were mounted on microscope slides coated with poly-L-lysine for enhanced attachment to the slide. They were covered with a glass coverslip while slightly immersed in water. The slides were placed on a frozen metal block at −80 °C for 30 min. The coverslip was rapidly removed from the slide ('freeze-crack') and the sample was immediately fixed in −20 °C methanol for 2 min, followed by a cold wash in PBS and a 10-min incubation in 4% formaldehyde with PBS. The samples are subsequently washed twice in PBS then with 10% formamide in 2x SSC buffer.

The hybridization mix consisted of 10% formamide, 10 mM vanadyl ribonucleoside complex, 1 mg/ml *E. Coli* tRNAs, 200 μg/ml BSA, 0.1 mg/ml dextran sulfate, 2x SSC and 125 nM probes. The samples were immersed in the hybridization mix and incubated overnight at 37 °C enclosed in a humidified hybridization chamber. The slides were washed twice in 2x SSC buffer and incubated in preheated 10% formamide in 2x SSC buffer (37 °C) for 30 min. Then they were rinsed twice in 2x SSC buffer and stained with 0.1 μg/ml DAPI for 10 min. After 2 rinses in 2x SSC buffer, the samples were mounted in Vectashield mounting media and sealed with nail polish.

Images were acquired on a Nikon Ti2E microscope equipped with a 100 × 1.45 NA objective and an Andor Ikon-M high sensitivity camera using NIS (Nikon Imaging Software). Images were acquired as z-stacks with step size of 0.5 μm. mRNA numbers were quantified using a previously developed MATLAB script (Katsanos et al., 2017). This semi-automated script allows manual selection of the region of interest (ROI) by drawing the outlines of the selected cell across the z-stacks. The script prompts an interactive threshold selection, and based on this threshold, automatically counts the number of mRNA spots in three dimensions.

2.3. Imaging of axonal projections

The analyses of AIY axons at L4 larval stage were performed using a Nikon Ti2E epifluorescence microscope equipped with a Hamamatsu ORCA-Flash 4.0 camera and NIS (Nikon Imaging Software). The characterizations at 3-fold embryonic stage were performed with a Nikon Ti microscope equipped with a Yokogawa CSU-X1 spinning disc module, a 480 nm laser, and a Photometrics Evolve EMCCD camera. Embryos and larvae were mounted on a 5% agar pad between a slide and a coverslip. Images were analyzed using Fiji.

2.4. Bioinformatic analysis of scRNA-seq expression data

The scRNA-seq data were obtained from (Packer et al., 2019). We used the raw gene-by-cell count matrix. Background corrected UMI counts were used as a measure of gene expression. In order to identify genes with left-right asymmetric expression in the AIY lineage, we first estimated which cells are left or right. As the scRNA-seq data lack left-right annotation in the AIY lineage, we used our prior knowledge that *hlh-16* is enriched in the left cells of the AIY lineage. First, we extracted from the dataset cells belonging to the AIY lineage. Specifically, we selected the grandmother and mother cells of the AIY neuron, as they have high levels of *hlh-16* expression. The annotation used to identify AIY grandmother cell is ABpl/rpapaa and for AIY mother cell is ABpl/rpapaaa. For each of the 282 cells that were obtained, *hlh-16* expression was normalized with *ref-2*, a gene that is symmetrically expressed in the AIY lineage and with a timing similar to *hlh-16*. The cells were binned into the four time windows present in the annotation (Packer et al., 2019): 170–210, 210–270, 270–330, 330–390 min post first cleavage. For each time window, we calculated the mean normalized expression level of *hlh-16*. The cells with *hlh-16* level higher than the mean were classified as left cells in the given time window, and those with *hlh-16* level lower than the mean were classified as right cells. Then for each gene in the scRNA-seq dataset, we normalized the gene expression with *ref-2* and calculated its mean expression in the left and right cells. We compared the left and right means of the given gene using Mann-Whitney U statistical tests. If a gene had a significantly higher ($p < 0.05$) expression level on one side in several time windows, we considered this gene as a potential candidate with left-right asymmetric expression in the AIY lineage. Out of 20,222 genes in the scRNA-seq dataset, this analysis identified only 6 genes with L-R asymmetric expression in at least 3 of the 4 time bins. One is *fmi-1* (a Flamingo ortholog and good candidate in regulation of axon growth) and the others are *chk-1* (a mitotic checkpoint kinase), *htz-1* (a histone), *prp-17* (a splicing factor), *ubc-16* (a ubiquitin conjugating enzyme) and *Y104H12D.2* (uncharacterized). We also performed a similar analysis with normalization with total UMI instead of *ref-2*, and observed only 25 genes with L-R asymmetric expression in at least 2 of the 4 time bins. *fmi-1* is again one of them.

2.5. Statistics

The raw numerical data used to generate the graphs are in Table S2. GraphPad Prism was used for statistical analyses. Comparisons of the asymmetry index to 1 were performed using a non-parametric two-tailed Wilcoxon signed-rank test. For comparisons of proportions, a two-tailed Fisher's exact test was used. Analyses of expression levels were performed with a non-parametric two-tailed Mann-Whitney *U* test. The test used, p-value obtained and numbers of animals or cells analyzed are presented in the figures and figure legends.

3. Results

3.1. efn-2 is asymmetrically expressed and regulated by hlh-16

We have previously observed that the transcription factor *hlh-16* is L-R asymmetrically expressed in the AIY neuron lineage using transcriptional and translational fluorescent reporter fusions (Bertrand et al., 2011). To determine whether single-molecule fluorescence *in situ* hybridization (smFISH) can be used to detect L-R asymmetry of expression in the AIY lineage, we selected *hlh-16* as a test case. smFISH allows the quantification of the number of mRNA molecules of a specific gene of interest (Bordet et al., 2022; Raj et al., 2008). As mRNA numbers quickly change over time during development, to assess L-R asymmetry in expression, we measured in each embryo the asymmetry index defined as the number of mRNAs in the left cell divided by the mean number of mRNAs of the two cells. Thus, this index varies between 2 (for a gene

expressed only in the left cell) and 0 (for a gene expressed only in the right cell), with a value of 1 for a symmetrically expressed gene. smFISH analysis reveals endogenous *hlh-16* expression in the AIY grandmother cells (Fig. 1B) with an asymmetry index statistically higher than 1 (Fig. 1C). This confirms the left enrichment previously observed with fluorescent reporters (Bertrand et al., 2011).

HLH-16 regulates AIY axon projections in a L-R asymmetric manner, however the axon guidance molecules acting downstream of HLH-16 remain to be identified. Ephrins are evolutionarily conserved axon guidance proteins (Miller and Chin-Sang, 2012) and it was previously suggested that the ephrin gene *efn-2* could be asymmetrically expressed in the AIY lineage using a transcriptional fluorescent reporter (Grossman et al., 2013). With smFISH, we observed that the endogenous *efn-2* gene is expressed in the AIY mother cell (Fig. 1D) with a significantly stronger level in the left cell (Fig. 1E). By contrast, for the symmetrically expressed transcription factor gene *ttx-3* (Bertrand and Hobert, 2009; Bordet et al., 2022; Filippopoulou et al., 2021), we observed a symmetric signal by smFISH (Fig. 1F). As *hlh-16* is expressed before *efn-2* in the AIY lineage and with a similar L-R asymmetry, we tested whether *hlh-16* could regulate *efn-2* asymmetry. In *hlh-16(ot711)* loss-of-function mutants (likely null allele, see Table S3 for allele description), we observed that *efn-2* is still expressed in the AIY mother cells but in a L-R symmetric manner (Fig. 1E). Taken together, these data suggest that *efn-2* is asymmetrically expressed in the AIY lineage and that this asymmetry is regulated by *hlh-16*.

There are three other *ephrin* genes in the *C. elegans* genome: *vab-2, efn-3* and *efn-4* (Miller and Chin-Sang, 2012). scRNA-seq data that cover *C. elegans* embryonic development (Packer et al., 2019) suggest that *efn-4* is expressed in postmitotic AIY and *vab-2* in postmitotic SMDD, while *efn-3* is not expressed. We confirmed this using smFISH and observed no statistically significant L-R asymmetry for *efn-4* in AIY or *vab-2* in SMDD (Figs. S1A–D).

3.2. *efn-2 has an asymmetric effect on AIY axons*

The left and right AIY neurons have symmetric axons that can be visualized using a *ttx-3p::gfp* transgene at L4 larval stage. Starting from the cell body, the AIY axon extends anteriorly, then turns dorsally entering the nerve ring (the main *C. elegans* neuropil) and stops at the dorsal midline (Fig. 2A). In *hlh-16* loss-of function mutants, the AIY axon stops prematurely, before reaching the dorsal midline (Fig. 2A) (Bertrand et al., 2011). This phenotype is partially penetrant and the proportion of neurons showing axonal defects is higher for the left AIY than the right AIY (Fig. 2B) (Bertrand et al., 2011). As *efn-2* is L-R asymmetrically expressed and regulated by *hlh-16*, we tested whether *efn-2* regulates AIY axonal projections. However, we did not observe AIY axonal defects in *efn-2(ev658)* loss-of-function mutants (likely null allele) (Fig. 2B). It has been previously shown that *efn-4* regulates AIY axonal projection (Schwieterman et al., 2016), however, whether the effect is L-R asymmetric was not analyzed. In *efn-4(bx80)* loss-of-function mutants (likely null allele) we observed that the AIY axon stops prematurely with a similar penetrance for AIYL and AIYR (Fig. 2B). Interestingly, the *efn-2* mutation increases these axonal defects specifically in AIYL (Fig. 2B). We concluded that *efn-2* has an asymmetric effect on AIY axonal projections that mirrors its asymmetric expression, while *efn-4* has a symmetric effect echoing its symmetric expression. We also tested the effect of a loss-of-function mutation (likely null allele) for the third ephrin expressed in the lineage, *vab-2 (ju1)*, but did not observe any strong defect even when combined with the *efn-2(ev658)* mutation.

AIY axons grow during embryogenesis (Moyle et al., 2021; Rapti et al., 2017). To determine if the axonal phenotype that we observed is

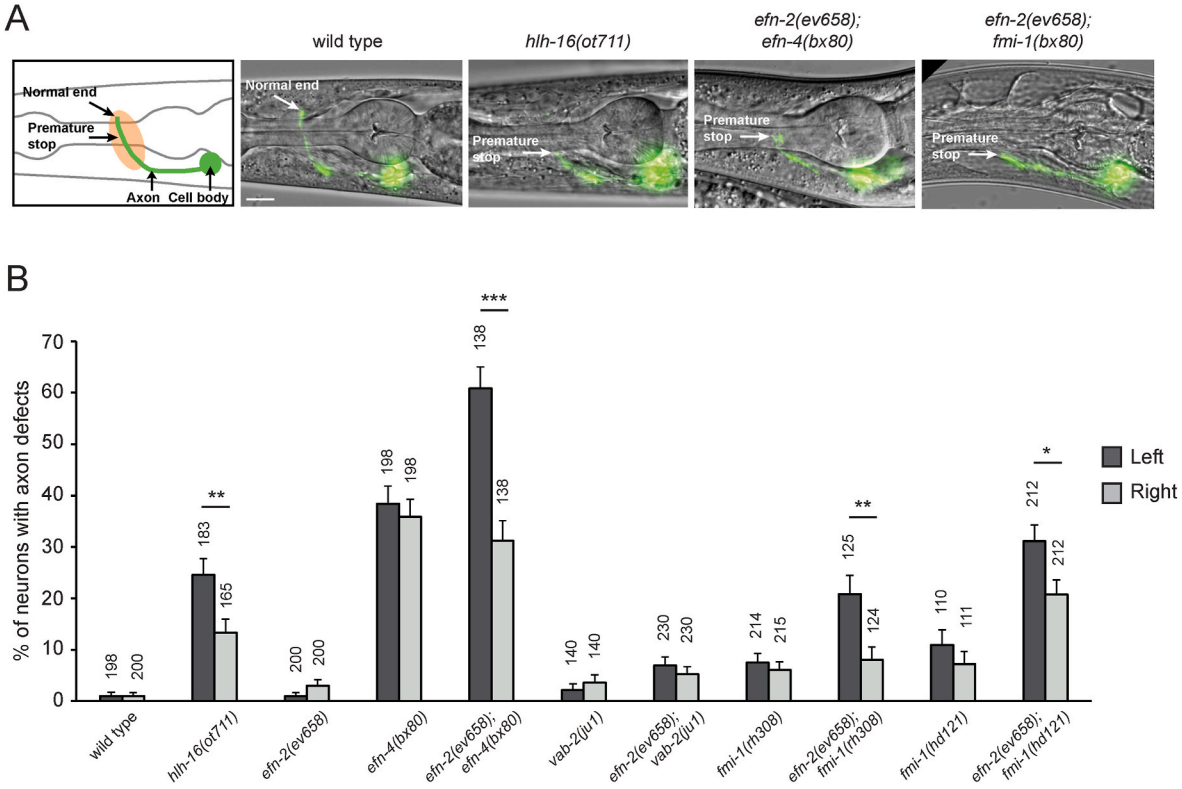

Fig. 2. Effect of *ephrin* and *fmi-1* mutants on AIY axon at larval stage.
(A) Lateral view of the head region of L4 larvae with the AIY axon visualized with *ttx-3p::gfp*. In wild-type animals, the axon ends at the dorsal midpoint of the nerve ring (nerve ring area in orange). In mutants, the axon often stops prematurely. Anterior is left, dorsal is up, scale bar: 10 μm. (B) Percentage of left or right AIY neurons, which express *ttx-3p::gfp*, showing axonal projection defects (premature stop) in wild-type or mutant animals at late larval stage (L4). Error bars show standard error of proportion; numbers above the bars show numbers of GFP-positive neurons analyzed; Fisher's exact test (***p < 0.005, **p < 0.01, *p < 0.05).

due to defects in the development or the maintenance of the axons, we looked at 3-fold stage embryos, the earliest stage at which AIY axons can be unambiguously visualized with the *ttx-3p::gfp* transgene. We observed that the axonal phenotype of *efn-2(ev658); efn-4(bx80)* double mutants is already present in the embryos (Fig. 3A and B), suggesting that the defects occur during axonal development.

3.3. *fmi-1 is asymmetrically expressed and regulated by hlh-16*

To identify other genes that could be asymmetrically expressed and cooperate with *efn-2* in regulating AIY axonal growth, we analyzed scRNA-seq data that cover *C. elegans* embryogenesis (Packer et al., 2019). We analyzed data of single cells annotated as AIY grandmother cells or AIY mother cells in four time bins. Simple clustering did not separate left from right cells (Packer et al., 2019), probably because their transcription profiles are too similar. To identify genes that may show an enrichment in the left AIY lineage, we separated the cells into high *hlh-16*-expressing and low *hlh-16*-expressing after normalizing with *ref-2*, a gene transcribed with the same timing as *hlh-16* but in a L-R symmetric manner (see materials and methods). This analysis identified only 6 genes with L-R asymmetric expression in at least 3 of the 4 time bins, one being *fmi-1* (Fig. 4A). FMI-1 is an atypical cadherin of the Flamingo/CELSR family that has been shown to regulate axon guidance in *C. elegans* (Chisholm et al., 2016) and is therefore a good candidate to regulate AIY L-R asymmetric axonal growth. The 5 other genes are *chk-1* (a mitotic checkpoint kinase), *htz-1* (a histone), *prp-17* (a splicing factor), *ubc-16* (a ubiquitin conjugating enzyme) and *Y104H12D.2* (uncharacterized).

To confirm that *fmi-1* is asymmetrically expressed, we analyzed its expression with smFISH. We observed that *fmi-1* is expressed in the AIY mother cells (Fig. 4B) and enriched in the left cell (Fig. 4C). Interestingly, this L-R asymmetry is lost in *hlh-16(ot711)* loss-of-function mutants, showing that this asymmetry is also regulated by *hlh-16*.

3.4. *fmi-1 has an asymmetric effect on AIY axons when combined with efn-2*

We then tested the effect of *fmi-1* loss-of-function alleles, *rh308* and *hd121* (likely null alleles), on AIY axons at L4 larval stage (Fig. 2). We observed that *fmi-1(rh308)* and *fmi-1(hd121)* display a weak axonal defect phenotype that is increased and becomes asymmetric when combined with the *efn-2(ev658)* mutation. The phenotype of *fmi-1; efn-2* double mutants is similar to that of *hlh-16(ot711)* mutants. In addition, we observed that the axonal phenotype of *fmi-1; efn-2* double mutants is

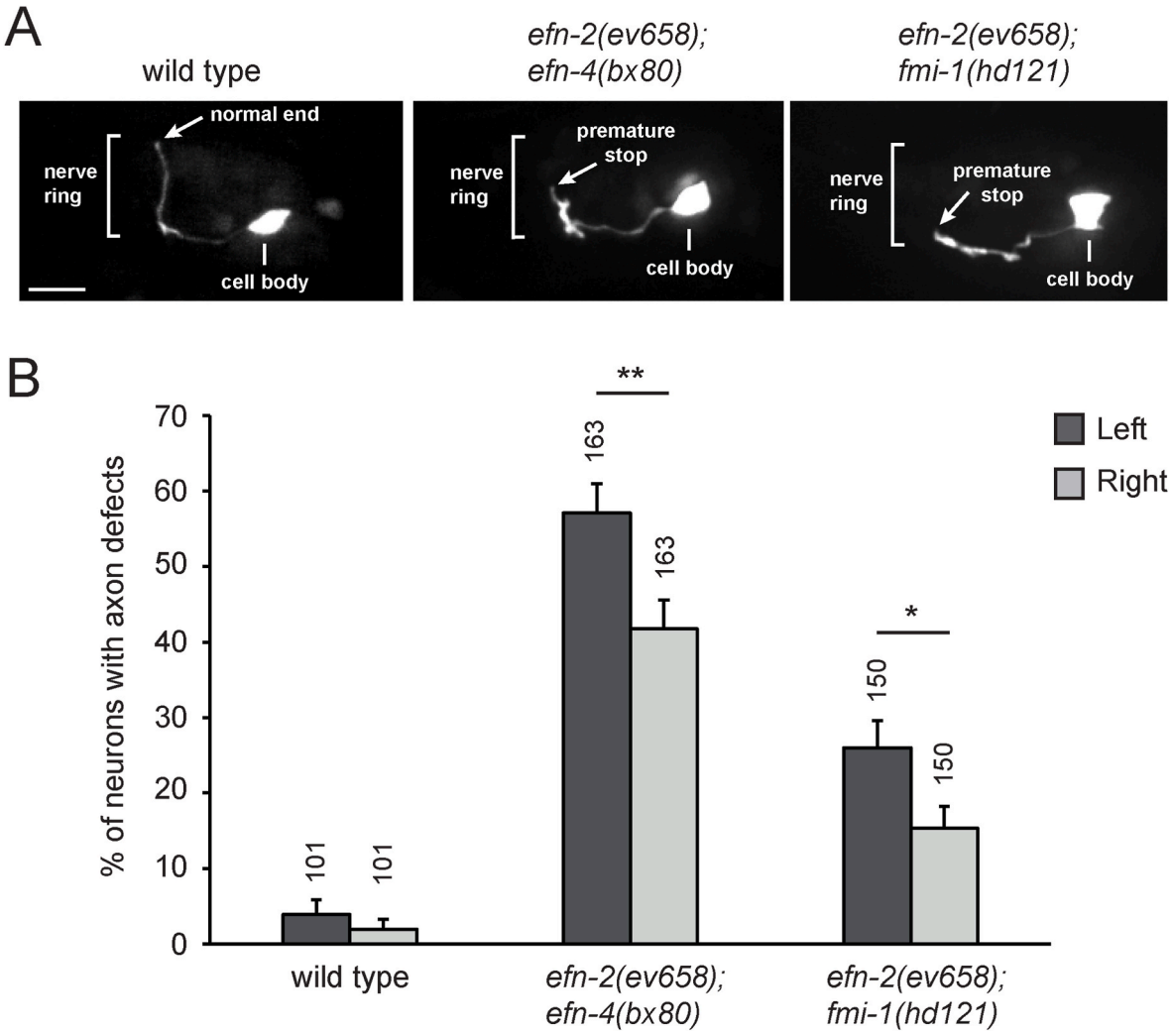

Fig. 3. Effect of *ephrin* and *fmi-1* mutants on AIY axon at embryonic stage.
(A) Lateral view of the head region of 3-fold embryos with the AIY axon visualized with *ttx-3p::gfp*. In wild-type animals, the axon ends at the dorsal midpoint of the nerve ring. In mutants, the axon often stops prematurely. Anterior is left, dorsal is up, scale bar: 5 μm. (B) Percentage of left or right AIY neurons, which express *ttx-3p::gfp*, showing axonal projection defects (premature stop) in wild-type or mutant animals at 3-fold embryonic stage. Error bars show standard error of proportion; numbers above the bars show numbers of GFP-positive neurons analyzed; Fisher's exact test (**$p < 0.01$, *$p < 0.05$).

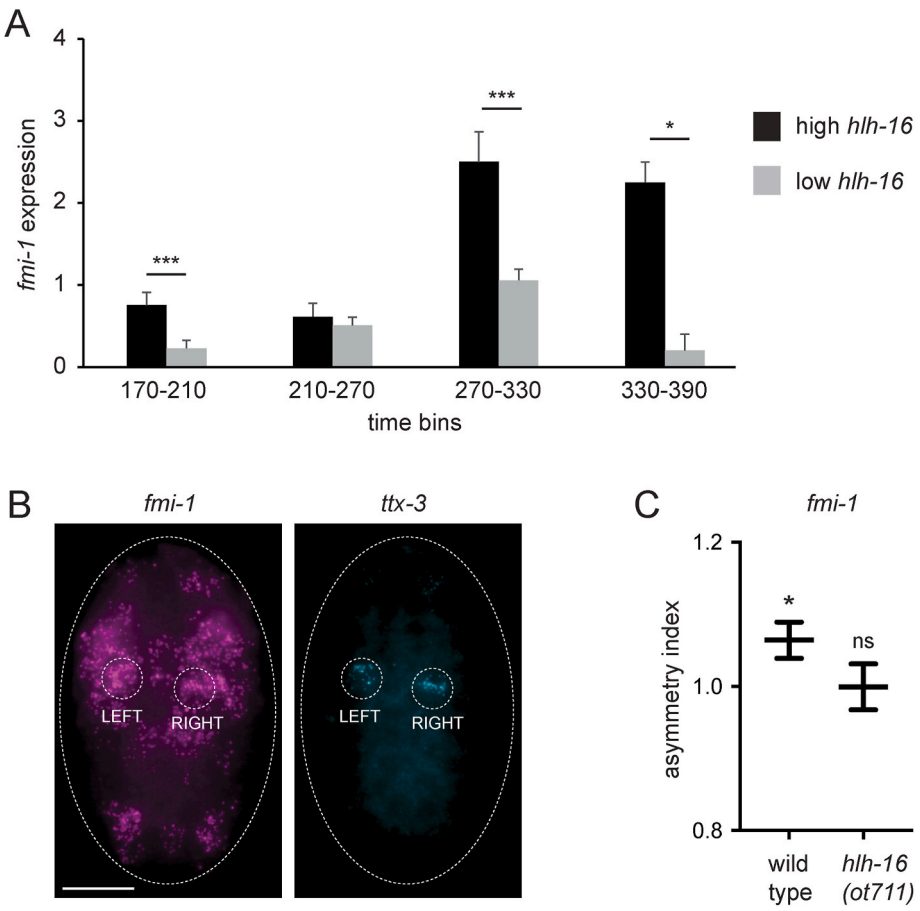

Fig. 4. *fmi-1* is asymmetrically expressed in the AIY lineage.
(A) *fmi-1* expression from scRNA-seq data. Mean *fmi-1* expression normalized with *ref-2* in the AIY grandmother cells and mother cells in four time bins (in minutes post first cleavage). Cells are separated in high *hlh-16*-expressing and low *hlh-16*-expressing. Respective numbers of cells per time bin: 62, 73, 138 and 9. Error bars represent the SEM. Mann-Whitney *U* test (***p < 0.005, *p < 0.05). (B) Image of an embryo labeled with smFISH targeting *fmi-1* mRNAs (Quasar 670) and *ttx-3* mRNAs (CAL Fluor Red 610). *ttx-3* was used to identify the AIY mother cells. Left and right AIY mother cells are circled, anterior is up, scale bar: 10 μm. (C) Asymmetry index of *fmi-1* mRNA numbers detected by smFISH in the AIY mother cell. n = 30 embryos analyzed for wild-type and 30 embryos for *hlh-16(ot711)* mutants, bars represent the mean and SEM, comparison to 1 using Wilcoxon signed-rank test (*p < 0.05, ns - not significant).

already present in 3-fold embryos (Fig. 3), suggesting that the defects occur during axonal development. Taken together, these data indicate that *efn-2* and *fmi-1* cooperate to regulate AIY axonal projections in a L-R asymmetric manner and downstream of *hlh-16*.

3.5. *EFN-2 may act via a non-canonical receptor, SAX-7*

FMI-1 is a transmembrane protein that interacts homophilically with FMI-1 on neighboring cells (Berger-Muller and Suzuki, 2011). In contrast, ephrins are membrane-bound proteins that interact with other types of transmembrane proteins on neighboring cells in a heterophilic manner, potentially leading to bidirectional signaling (Miller and Chin-Sang, 2012). We therefore looked for potential ephrin interactors that could play a role in asymmetric AIY axonal regulation. In *C. elegans*, there is one canonical ephrin receptor of the EphR family, VAB-1 (Miller and Chin-Sang, 2012). However, *vab-1(dx31)* loss-of-function mutants (likely null allele) do not show the AIY axonal defects observed in *efn-2; efn-4* double mutants (Figs. 5B and 2B). It has been previously observed that the L1CAM transmembrane proteins, LAD-2 and SAX-7, can act as alternative non-canonical ephrin receptors in *C. elegans* (Dong et al., 2016). We observed that *lad-2(tm3056)* mutants (likely null allele) or *sax-7(nj48)* mutants (strong loss-of-function allele) do not display the phenotype of *efn-2; efn-4* double mutants, even when the *lad-2* and *sax-7* mutations are combined (Fig. 5B). Finally, even the triple mutant *vab-1 (dx31); lad-2(tm3056); sax-7(nj48)* fails to phenocopy the *efn-2; efn-4* double mutant (Fig. 5B).

We reasoned that EFN-2 and EFN-4 may act via different receptors in the regulation of AIY axonal growth. SAX-3, a member of the ROBO family of transmembrane proteins, has been shown to physically bind EFN-4 and to act as a potential ephrin co-receptor in *C. elegans* (Ghenea et al., 2005; Nawrocka et al., 2024). We therefore analyzed the effect of the *sax-3(ky123)* loss-of-function allele (likely null) and observed a strong symmetric axonal phenotype similar to the one of *efn-4(bx80)* single mutants (Figs. 5B and 2B). This suggests that SAX-3 could be the interactor of EFN-4 during AIY axonal growth. To identify potential interactors for EFN-2, we used the fact that *efn-2* loss-of-function mutants enhance the phenotype of *fmi-1* mutants (Fig. 2B). We observed a similar enhancement of the *fmi-1* phenotype with *sax-7(nj48)*, but not with *vab-1(dx31)* or *lad-2(tm3056)* (Fig. 5B). This suggests that SAX-7 could be the interactor of EFN-2 in the regulation of AIY axons.

Finally, we noticed that the mutants displaying L-R asymmetric axonal phenotypes (*hlh-16* single, *efn-2; efn-4* double, *efn-2; fmi-1* double and *fmi-1; sax-7* double) (Figs. 2B and 5B) have statistically significant defects in both left and right axons when compared to wild-type animals (see Table S4 for additional statistics). Both the left and right AIY are affected but the effect is stronger on the left side. This indicates that HLH-16, EFN-2 and FMI-1 regulate both AIYL and AIYR axons, and that the level of requirement is higher in AIYL mirroring their higher expression on the left side.

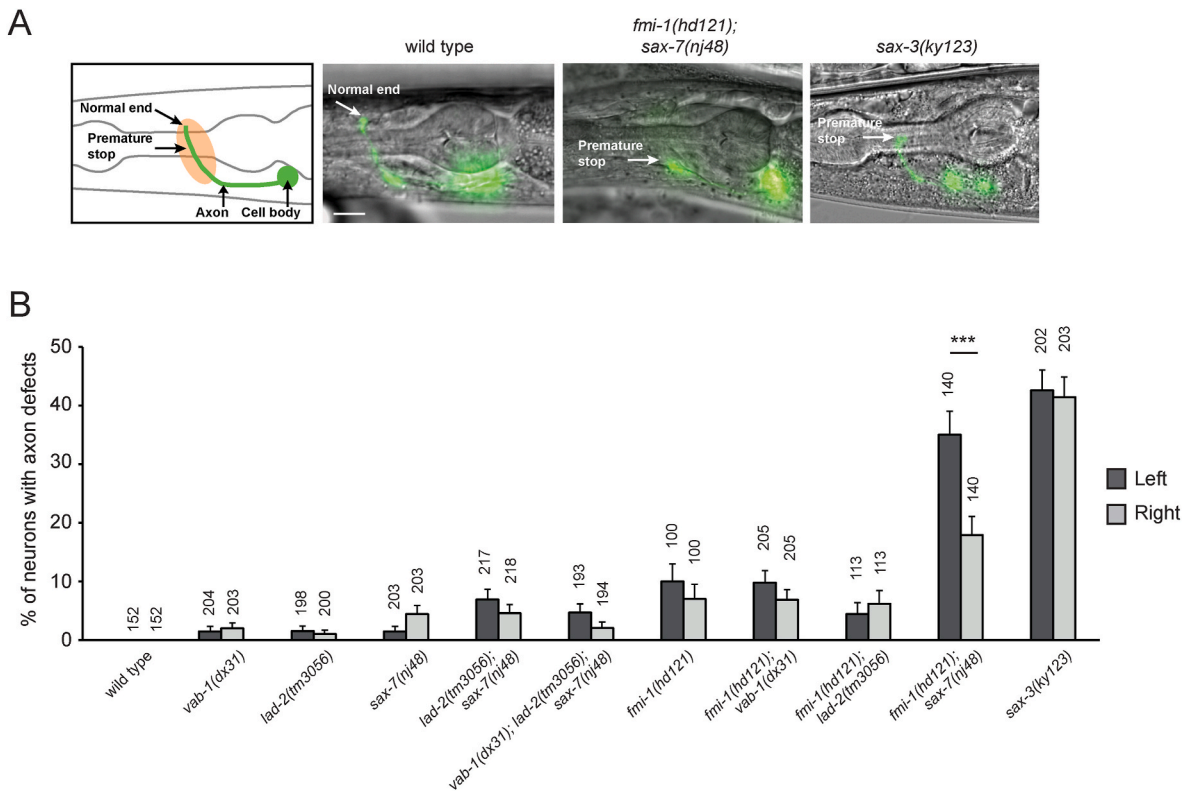

Fig. 5. Effect of *ephrin receptor* mutants on AIY axon at larval stage.
(A) Lateral view of the head region of L4 larvae with the AIY axon visualized with *ttx-3p::gfp*. In wild-type animals, the axon ends at the dorsal midpoint of the nerve ring (nerve ring area in orange). In mutants, the axon often stops prematurely. Anterior is left, dorsal is up, scale bar: 10 μm. (B) Percentage of left or right AIY neurons, which express *ttx-3p::gfp*, showing axonal projection defects (premature stop) in wild-type or mutant animals at late larval stage (L4). Error bars show standard error of proportion; numbers above the bars show numbers of GFP-positive neurons analyzed; Fisher's exact test (***$p < 0.005$).

4. Discussion

In this study, we have identified a L-R asymmetric program regulating axonal growth downstream of the transcription factor HLH-16. We have shown that HLH-16 induces the asymmetric expression of two axon guidance molecules, EFN-2 and FMI-1 in the AIY lineage. In *efn-2*; *fmi-1* double mutants, we observed that AIY axons stop prematurely and that AIYL is more affected than AIYR, which is similar to the phenotype of *hlh-16* mutants. This suggests that higher levels of EFN-2 and FMI-1 are required in the left AIY lineage for correct axonal projection.

The left and right AIY axons are symmetric in wild-type animals raising the question of why do *efn-2; fmi-1* mutants display an asymmetric phenotype. One possibility is that the AIYL and AIYR axons have to navigate slightly different environments and therefore require different EFN-2 and FMI-1 levels for correct projection. Indeed, the environments of the left and right AIY neurons are not identical. For instance, the unilateral neuron RIS is present only on the right side in close proximity to AIYR, while the excretory cell soma is located on the left side close to AIYL (Sulston et al., 1983). These differences in cellular neighborhood may create distinct mechanical constraints between the two sides. In addition, by secreting molecules, these unilateral cells may also generate different chemical environments on the left and right sides. It is therefore possible that the left side is more challenging for the AIY axon to navigate than the right side and requires higher EFN-2 and FMI-1 expression. In other words, the asymmetry of EFN-2 and FMI-1 expression in the AIY lineage compensates for an asymmetry in the navigation environment.

The nerve ring is built in a sequential manner. Eight pairs of pioneer neurons (including SMDD, SIAD and SIBV) send their axonal projections first, followed by follower neurons (including AIY) (Moyle et al., 2021; Rapti et al., 2017). In *fmi-1* mutants, the projection of pioneer axons is not affected (Rapti et al., 2017). Flamingo proteins act in a homophilic manner promoting adhesion between neighboring cells (Berger-Muller and Suzuki, 2011). It has been observed that, in the ventral nerve cord, FMI-1 mediates adhesion between pioneer and follower axons (Steimel et al., 2010). It is therefore possible that, in a similar way, FMI-1 mediates adhesion between pioneer axons (including SMDD) and AIY axons. The higher expression of FMI-1 in the left SMDD and AIY neurons may promote higher adhesion between pioneer axons and AIY axons on the left side compensating for a more difficult navigation environment on the left side.

Moreover, we found that the L-R asymmetry in *fmi-1* expression is likely specific to the AIY lineage. As *fmi-1* is also expressed in many cells other than the AIY lineage in the embryo, we measured by smFISH the *fmi-1* asymmetry in the whole embryo (Fig. S1E). We did not observe a statistically significant asymmetry suggesting that *fmi-1* asymmetry is not global but lineage specific.

Ephrins are membrane associated proteins that interact with transmembrane proteins on neighboring cells and can signal in a bidirectional manner (Miller and Chin-Sang, 2012). Our data suggest that EFN-2 may interact with the L1CAM protein SAX-7 in the regulation of AIY axonal growth. The interaction between ephrins and L1CAM proteins has been observed as attractive during axon guidance (Dong et al., 2016). Antibody staining has shown that SAX-7 is ubiquitously expressed in the *C. elegans* embryo (Chen et al., 2001). In addition, we have observed that EFN-2 is expressed in both SMDD and AIY. The interaction between EFN-2 and SAX-7 may therefore promote the association between AIY axons and pioneer axons (including SMDD) during AIY axonal growth. The higher level of expression of EFN-2 in the left SMDD and AIY neurons may facilitate AIY navigation on the left side where traveling is harder.

The asymmetry, which we characterized here in the AIY neurons, is drastically different from the previously described asymmetries in ASE and AWC neurons. The degree of asymmetry seems higher in ASE and AWC that display batteries of genes expressed only on the left or right side (Alqadah et al., 2016; Hobert, 2014). In the AIY lineage the difference resides in the levels of expression rather than on-off expression. This lower asymmetry in AIY is consistent with the observation that a simple clustering approach can separate ASE and AWC neurons into left or right in scRNA-seq data analysis, while this is not the case for the AIY lineage (Packer et al., 2019; Taylor et al., 2021). In addition, the asymmetry in the AIY lineage seems to be transient. HLH-16 is only expressed in the embryo, where it regulates a brief axonal growth program. HLH-16 is no longer expressed in the AIY lineage at larval and adult stages, and there is no evidence of left-right asymmetries in AIY after embryogenesis. In contrast, ASE and AWC express chemoreceptors in an asymmetric manner from embryogenesis to adulthood, leading to permanent physiological asymmetries (Alqadah et al., 2016; Hobert, 2014).

L-R asymmetries in axonal projections are also observed in other animals. It has been shown in *Drosophila* that the bilateral H-neurons project asymmetrically in the central brain, a process regulated by the netrin pathway (Lapraz et al., 2023). In mice, the innervation of diaphragm muscles by left and right phrenic motoneurons is asymmetric and controlled by Robo signaling (Charoy et al., 2017). However, in these examples, the final axonal pattern is L-R asymmetric. Our study shows that even bilaterally symmetric axons can be generated via asymmetric developmental genetic programs. It seems therefore likely that many molecular asymmetries, hidden in bilateral symmetric neuronal structures, remain to be discovered.

Funding

This work was funded by a grant from the Fondation pour la Recherche Médicale (DEQ20180339160) to V.B. The project leading to this publication has received funding from France 2030, the French Government program managed by the French National Research Agency (ANR-16-CONV-0001) and from Excellence Initiative of Aix-Marseille University - AMIDEX. This work was supported by the Fondation ARC pour la recherche sur le cancer with a fellowship (ARC-DOC42023020006287) to K.B. The funders had no role in study design, data collection and analysis, decision to publish, or preparation of the manuscript.

Declaration of interest

The authors declare that they have no known competing financial interests or personal relationships that could have appeared to influence the work reported in this paper.

CRediT authorship contribution statement

Khulganaa Buyannemekh: Writing – original draft, Visualization, Validation, Methodology, Investigation, Formal analysis, Conceptualization, Writing – review & editing. **Paul Villoutreix:** Writing – original draft, Visualization, Validation, Supervision, Methodology, Funding acquisition, Conceptualization, Writing – review & editing. **Vincent Bertrand:** Writing – review & editing, Writing – original draft, Visualization, Validation, Supervision, Project administration, Methodology, Funding acquisition, Formal analysis, Conceptualization.

Data availability

Data will be made available on request.

Acknowledgments

We thank members of our labs for comments on the manuscript. Imaging was performed on the PiCSL core facility (IBDM), member of the national infrastructure France-BioImaging supported by the French National Research Agency (ANR-10-INBS-04). Some strains were provided by the CGC, which is funded by NIH Office of Research Infrastructure Programs (P40OD010440).

Appendix A. Supplementary data

Supplementary data to this article can be found online at https://doi.org/10.1016/j.ydbio.2024.09.014.

References

Alqadah, A., Hsieh, Y.W., Xiong, R., Chuang, C.F., 2016. Stochastic left-right neuronal asymmetry in Caenorhabditis elegans. Philos. Trans. R. Soc. Lond. B Biol. Sci. 371. https://doi.org/10.1098/rstb.2015.0407.

Berger-Muller, S., Suzuki, T., 2011. Seven-pass transmembrane cadherins: roles and emerging mechanisms in axonal and dendritic patterning. Mol. Neurobiol. 44, 313–320. https://doi.org/10.1007/s12035-011-8201-5.

Bertrand, V., Bisso, P., Poole, R.J., Hobert, O., 2011. Notch-dependent induction of left/right asymmetry in C. elegans interneurons and motoneurons. Curr. Biol. 21, 1225–1231. https://doi.org/10.1016/j.cub.2011.06.016.

Bertrand, V., Hobert, O., 2009. Linking asymmetric cell division to the terminal differentiation program of postmitotic neurons in C. elegans. Dev. Cell 16, 563–575. https://doi.org/10.1016/j.devcel.2009.02.011.

Bolkova, J., Lanctot, C., 2016. Quantitative gene expression analysis in Caenorhabditis elegans using single molecule RNA FISH. Methods 98, 42–49. https://doi.org/10.1016/j.ymeth.2015.11.008.

Bordet, G., Couillault, C., Soulavie, F., Filippopoulou, K., Bertrand, V., 2022. PRC1 chromatin factors strengthen the consistency of neuronal cell fate specification and maintenance in C. elegans. PLoS Genet. 18, e1010209. https://doi.org/10.1371/journal.pgen.1010209.

Charoy, C., Dinvaut, S., Chaix, Y., Morle, L., Sanyas, I., Bozon, M., Kindbeiter, K., Durand, B., Skidmore, J.M., De Groef, L., et al., 2017. Genetic specification of left-right asymmetry in the diaphragm muscles and their motor innervation. Elife 6. https://doi.org/10.7554/eLife.18481.

Chen, L., Ong, B., Bennett, V., 2001. LAD-1, the Caenorhabditis elegans L1CAM homologue, participates in embryonic and gonadal morphogenesis and is a substrate for fibroblast growth factor receptor pathway-dependent phosphotyrosine-based signaling. J. Cell Biol. 154, 841–855. https://doi.org/10.1083/jcb.200009004.

Chisholm, A.D., Hutter, H., Jin, Y., Wadsworth, W.G., 2016. The genetics of axon guidance and axon regeneration in Caenorhabditis elegans. Genetics 204, 849–882. https://doi.org/10.1534/genetics.115.186262.

Concha, M.L., Bianco, I.H., Wilson, S.W., 2012. Encoding asymmetry within neural circuits. Nat. Rev. Neurosci. 13, 832–843. https://doi.org/10.1038/nrn3371.

Dong, B., Moseley-Alldredge, M., Schwieterman, A.A., Donelson, C.J., McMurry, J.L., Hudson, M.L., Chen, L., 2016. EFN-4 functions in LAD-2-mediated axon guidance in Caenorhabditis elegans. Development 143, 1182–1191. https://doi.org/10.1242/dev.128934.

Duboc, V., Dufourcq, P., Blader, P., Roussigne, M., 2015. Asymmetry of the brain: development and implications. Annu. Rev. Genet. 49, 647–672. https://doi.org/10.1146/annurev-genet-112414-055322.

Filippopoulou, K., Couillault, C., Bertrand, V., 2021. Multiple neural bHLHs ensure the precision of a neuronal specification event in C. elegans. Biol Open 10, bio058976. https://doi.org/10.1242/bio.058976.

Geminard, C., Gonzalez-Morales, N., Coutelis, J.B., Noselli, S., 2014. The myosin ID pathway and left-right asymmetry in Drosophila. Genesis 52, 471–480. https://doi.org/10.1002/dvg.22763.

Ghenea, S., Boudreau, J.R., Lague, N.P., Chin-Sang, I.D., 2005. The VAB-1 Eph receptor tyrosine kinase and SAX-3/Robo neuronal receptors function together during C. elegans embryonic morphogenesis. Development 132, 3679–3690. https://doi.org/10.1242/dev.01947.

Grossman, E.N., Giurumescu, C.A., Chisholm, A.D., 2013. Mechanisms of ephrin receptor protein kinase-independent signaling in amphid axon guidance in Caenorhabditis elegans. Genetics 195, 899–913. https://doi.org/10.1534/genetics.113.154393.

Gunturkun, O., Ocklenburg, S., 2017. Ontogenesis of lateralization. Neuron 94, 249–263. https://doi.org/10.1016/j.neuron.2017.02.045.

Hobert, O., 2014. Development of left/right asymmetry in the Caenorhabditis elegans nervous system: from zygote to postmitotic neuron. Genesis 52, 528–543. https://doi.org/10.1002/dvg.22747.

Hobert, O., Johnston Jr., R.J., Chang, S., 2002. Left-right asymmetry in the nervous system: the Caenorhabditis elegans model. Nat. Rev. Neurosci. 3, 629–640. https://doi.org/10.1038/nrn897.

Katsanos, D., Koneru, S.L., Boukhibar, L.M., Gritti, N., Ghose, R., Appleford, P.J., Doitsidou, M., Woollard, A., van Zon, J.S., Poole, R.J., Barkoulas, M., 2017. Stochastic loss and gain of symmetric divisions in the C. elegans epidermis perturbs robustness of stem cell number. PLoS Biol. 15, e2002429. https://doi.org/10.1371/journal.pbio.2002429.

Lapraz, F., Boutres, C., Fixary-Schuster, C., De Queiroz, B.R., Placais, P.Y., Cerezo, D., Besse, F., Preat, T., Noselli, S., 2023. Asymmetric activity of NetrinB controls laterality of the Drosophila brain. Nat. Commun. 14, 1052. https://doi.org/10.1038/s41467-023-36644-4.

Miller, M.A., Chin-Sang, I.D., 2012. Eph receptor signaling in C. elegans. WormBook 1–17. https://doi.org/10.1895/wormbook.1.151.1.

Moyle, M.W., Barnes, K.M., Kuchroo, M., Gonopolskiy, A., Duncan, L.H., Sengupta, T., Shao, L., Guo, M., Santella, A., Christensen, R., et al., 2021. Structural and developmental principles of neuropil assembly in C. elegans. Nature 591, 99–104. https://doi.org/10.1038/s41586-020-03169-5.

Nawrocka, W.I., Cheng, S., Hao, B., Rosen, M., Cortés, E., Baltrusaitis, E., Aziz, Z., Kovács, I.A., Özkan, E., 2024. Nematode extracellular protein interactome expands connections between signaling pathways. bioRxiv 2024.2007.2008, 602367. https://doi.org/10.1101/2024.07.08.602367.

Packer, J.S., Zhu, Q., Huynh, C., Sivaramakrishnan, P., Preston, E., Dueck, H., Stefanik, D., Tan, K., Trapnell, C., Kim, J., et al., 2019. A lineage-resolved molecular atlas of C. elegans embryogenesis at single-cell resolution. Science 365, eaax1971. https://doi.org/10.1126/science.aax1971.

Raj, A., van den Bogaard, P., Rifkin, S.A., van Oudenaarden, A., Tyagi, S., 2008. Imaging individual mRNA molecules using multiple singly labeled probes. Nat. Methods 5, 877–879. https://doi.org/10.1038/nmeth.1253.

Rapti, G., Li, C., Shan, A., Lu, Y., Shaham, S., 2017. Glia initiate brain assembly through noncanonical Chimaerin-Furin axon guidance in C. elegans. Nat. Neurosci. 20, 1350–1360. https://doi.org/10.1038/nn.4630.

Schwieterman, A.A., Steves, A.N., Yee, V., Donelson, C.J., Bentley, M.R., Santorella, E.M., Mehlenbacher, T.V., Pital, A., Howard, A.M., Wilson, M.R., et al., 2016. The Caenorhabditis elegans ephrin EFN-4 functions non-cell autonomously with heparan sulfate proteoglycans to promote axon outgrowth and branching. Genetics 202, 639–660. https://doi.org/10.1534/genetics.115.185298.

Steimel, A., Wong, L., Najarro, E.H., Ackley, B.D., Garriga, G., Hutter, H., 2010. The Flamingo ortholog FMI-1 controls pioneer-dependent navigation of follower axons in C. elegans. Development 137, 3663–3673. https://doi.org/10.1242/dev.054320.

Stiernagle, T., 2006. Maintenance of C. elegans. WormBook, pp. 1–11. https://doi.org/10.1895/wormbook.1.101.1.

Sulston, J.E., Horvitz, H.R., 1977. Post-embryonic cell lineages of the nematode, Caenorhabditis elegans. Dev. Biol. 56, 110–156. https://doi.org/10.1016/0012-1606(77)90158-0.

Sulston, J.E., Schierenberg, E., White, J.G., Thomson, J.N., 1983. The embryonic cell lineage of the nematode Caenorhabditis elegans. Dev. Biol. 100, 64–119. https://doi.org/10.1016/0012-1606(83)90201-4.

Sun, T., Walsh, C.A., 2006. Molecular approaches to brain asymmetry and handedness. Nat. Rev. Neurosci. 7, 655–662. https://doi.org/10.1038/nrn1930.

Taylor, S.R., Santpere, G., Weinreb, A., Barrett, A., Reilly, M.B., Xu, C., Varol, E., Oikonomou, P., Glenwinkel, L., McWhirter, R., et al., 2021. Molecular topography of an entire nervous system. Cell 184, 4329–4347. https://doi.org/10.1016/j.cell.2021.06.023.

White, J.G., Southgate, E., Thomson, J.N., Brenner, S., 1986. The structure of the nervous system of the nematode Caenorhabditis elegans. Philos. Trans. R. Soc. Lond. B Biol. Sci. 314, 1–340. https://doi.org/10.1098/rstb.1986.0056.